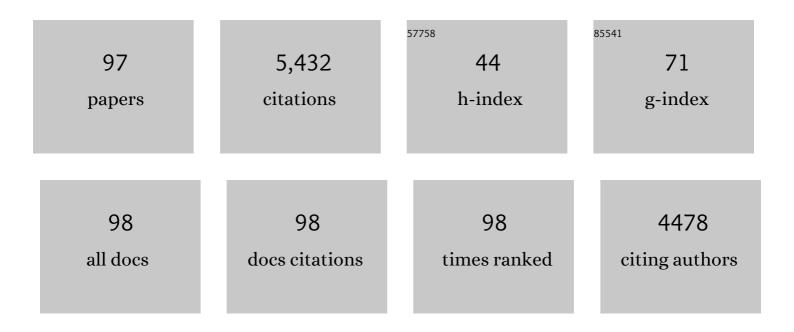
List of Publications by Year in descending order

Source: https://exaly.com/author-pdf/735349/publications.pdf Version: 2024-02-01



INF-HUNKIM

#	Article	IF	CITATIONS
1	Selective CO gas sensing by Au-decorated WS2-SnO2 core-shell nanosheets on flexible substrates in self-heating mode. Sensors and Actuators B: Chemical, 2022, 353, 131197.	7.8	17
2	Au-Decorated 1D SnO2 Nanowire/2D WS2 Nanosheet Composite for CO Gas Sensing at Room Temperature in Self-Heating Mode. Chemosensors, 2022, 10, 132.	3.6	8
3	Hydrogen sensing characteristics of Pd-decorated ultrathin ZnO nanosheets. Sensors and Actuators B: Chemical, 2021, 329, 129222.	7.8	35
4	Synergistic effects of SnO2 and Au nanoparticles decorated on WS2 nanosheets for flexible, room-temperature CO gas sensing. Sensors and Actuators B: Chemical, 2021, 332, 129493.	7.8	79
5	Synergistic Effects of Au and SnO2 Nanoparticles Decorated on WS2 Nanosheets for Flexible, Room-Temperature CO Gas Sensing. ECS Meeting Abstracts, 2021, MA2021-01, 1431-1431.	0.0	0
6	Achievement of self-heated sensing of hazardous gases by WS2 (core)–SnO2 (shell) nanosheets. Journal of Hazardous Materials, 2021, 412, 125196.	12.4	17
7	How femtosecond laser irradiation can affect the gas sensing behavior of SnO2 nanowires toward reducing and oxidizing gases. Sensors and Actuators B: Chemical, 2021, 342, 130036.	7.8	8
8	Chemical-recognition-driven selectivity of SnO2-nanowire-based gas sensors. Nano Today, 2021, 40, 101265.	11.9	25
9	Electrowetting-on-dielectric behavior of micro-nano hierarchical SiO2 layers decorated with noble metals. Ceramics International, 2021, 47, 28312-28320.	4.8	5
10	Optimization of the surface coverage of metal nanoparticles on nanowires gas sensors to achieve the optimal sensing performance. Sensors and Actuators B: Chemical, 2020, 302, 127196.	7.8	44
11	Enhancement of gas sensing by implantation of Sb-ions in SnO2 nanowires. Sensors and Actuators B: Chemical, 2020, 304, 127307.	7.8	52
12	Variation of shell thickness in ZnO-SnO2 core-shell nanowires for optimizing sensing behaviors to CO, C6H6, and C7H8 gases. Sensors and Actuators B: Chemical, 2020, 302, 127150.	7.8	56
13	Electrowetting-on-dielectric characteristics of ZnO nanorods. Scientific Reports, 2020, 10, 14194.	3.3	15
14	Indium-implantation-induced enhancement of gas sensing behaviors of SnO2 nanowires by the formation of homo-core–shell structure. Sensors and Actuators B: Chemical, 2020, 321, 128475.	7.8	29
15	Pd-decorated Si nano-horns as sensitive and selective hydrogen gas sensors. Materials Research Bulletin, 2020, 132, 110985.	5.2	14
16	Gas-sensing behaviors of TiO2-layer-modified SnO2 quantum dots in self-heating mode and effects of the TiO2 layer. Sensors and Actuators B: Chemical, 2020, 310, 127870.	7.8	26
17	Flexible and low power CO gas sensor with Au-functionalized 2D WS2 nanoflakes. Sensors and Actuators B: Chemical, 2020, 313, 128040.	7.8	80
18	Pd-functionalized core-shell composite nanowires for self-heating, sensitive, and benzene-selective gas sensors. Sensors and Actuators A: Physical, 2020, 308, 112011.	4.1	15

#	Article	IF	CITATIONS
19	Incorporation of metal nanoparticles in soda-lime glass sensors for enhancing selective sensing. Sensors and Actuators B: Chemical, 2019, 296, 126673.	7.8	11
20	Sub-ppm Formaldehyde Detection by n-n TiO2@SnO2 Nanocomposites. Sensors, 2019, 19, 3182.	3.8	32
21	Gas Sensing Properties of Mg-Incorporated Metal–Organic Frameworks. Sensors, 2019, 19, 3323.	3.8	20
22	ppb-Level Selective Hydrogen Gas Detection of Pd-Functionalized In2O3-Loaded ZnO Nanofiber Gas Sensors. Sensors, 2019, 19, 4276.	3.8	39
23	Realization of H2S sensing by Pd-functionalized networked CuO nanowires in self-heating mode. Sensors and Actuators B: Chemical, 2019, 299, 126965.	7.8	54
24	Co3O4-loaded ZnO nanofibers for excellent hydrogen sensing. International Journal of Hydrogen Energy, 2019, 44, 27499-27510.	7.1	44
25	Selective H2S sensing without external heat by a synergy effect in self-heated CuO-functionalized SnO2-ZnO core-shell nanowires. Sensors and Actuators B: Chemical, 2019, 300, 126981.	7.8	42
26	An overview on how Pd on resistive-based nanomaterial gas sensors can enhance response toward hydrogen gas. International Journal of Hydrogen Energy, 2019, 44, 20552-20571.	7.1	91
27	Low-Voltage-Driven Sensors Based on ZnO Nanowires for Room-Temperature Detection of NO ₂ and CO Gases. ACS Applied Materials & Interfaces, 2019, 11, 24172-24183.	8.0	74
28	Realization of Au-decorated WS2 nanosheets as low power-consumption and selective gas sensors. Sensors and Actuators B: Chemical, 2019, 296, 126659.	7.8	81
29	Pd functionalization on ZnO nanowires for enhanced sensitivity and selectivity to hydrogen gas. Sensors and Actuators B: Chemical, 2019, 297, 126693.	7.8	70
30	Enhancement of CO and NO2 sensing in n-SnO2-p-Cu2O core-shell nanofibers by shell optimization. Journal of Hazardous Materials, 2019, 376, 68-82.	12.4	59
31	Gasochromic WO3 Nanostructures for the Detection of Hydrogen Gas: An Overview. Applied Sciences (Switzerland), 2019, 9, 1775.	2.5	49
32	Toluene- and benzene-selective gas sensors based on Pt- and Pd-functionalized ZnO nanowires in self-heating mode. Sensors and Actuators B: Chemical, 2019, 294, 78-88.	7.8	107
33	Design of supersensitive and selective ZnO-nanofiber-based sensors for H2 gas sensing by electron-beam irradiation. Sensors and Actuators B: Chemical, 2019, 293, 210-223.	7.8	103
34	Selective H2S-sensing performance of Si nanowires through the formation of ZnO shells with Au functionalization. Sensors and Actuators B: Chemical, 2019, 289, 1-14.	7.8	35
35	Highly efficient hydrogen sensors based on Pd nanoparticles supported on boron nitride coated ZnO nanowires. Journal of Materials Chemistry A, 2019, 7, 8107-8116.	10.3	114
36	Enhanced Hydrogen Detection in ppb-Level by Electrospun SnO2-Loaded ZnO Nanofibers. Sensors, 2019, 19, 726.	3.8	27

#	Article	IF	CITATIONS
37	A Novel X-Ray Radiation Sensor Based on Networked SnO2 Nanowires. Applied Sciences (Switzerland), 2019, 9, 4878.	2.5	10
38	Improving the hydrogen sensing properties of SnO2 nanowire-based conductometric sensors by Pd-decoration. Sensors and Actuators B: Chemical, 2019, 285, 358-367.	7.8	93
39	Combination of Pd loading and electron beam irradiation for superior hydrogen sensing of electrospun ZnO nanofibers. Sensors and Actuators B: Chemical, 2019, 284, 628-637.	7.8	56
40	Predictive gas sensor based on thermal fingerprints from Pt-SnO2 nanowires. Sensors and Actuators B: Chemical, 2019, 281, 670-678.	7.8	63
41	Enhancement of H2S sensing performance of p-CuO nanofibers by loading p-reduced graphene oxide papers. Sensors and Actuators B: Chemical, 2019, 281, 453-461. Effect of temperature on gas sensing properties of lithium mml:math xmlns:mml="http://www.w3.org/1998/Math/MathML" altimg="si1.gif"	7.8	71
42	overflow="scroll"> <mml:mrow><mml:mo stretchy="false">(</mml:mo><mml:mi) 0="" 1<="" etqq0="" overlock="" rgbt="" td="" tj=""><td>0 Tf 50 54 3.6</td><td>7 Td (mathva 19</td></mml:mi)></mml:mrow>	0 Tf 50 54 3.6	7 Td (mathva 19
43	xmlns:mml="http://www.w3.org/1998/Math/MathML" altimg="si2.gif" overflow="scroll"> <mml:mrow>< Design and fabrication of highly selective H2 sensors based on SIM-1 nanomembrane-coated ZnO nanowires. Sensors and Actuators B: Chemical, 2018, 264, 410-418.</mml:mrow>	7.8	37
44	Super anticorrosion of aluminized steel by a controlled Mg supply. Scientific Reports, 2018, 8, 3760.	3.3	3
45	Realization of superhydrophobic aluminum surfaces with novel micro-terrace nano-leaf hierarchical structure. Applied Surface Science, 2018, 451, 207-217.	6.1	26
46	CuO–TiO2 p–n core–shell nanowires: Sensing mechanism and p/n sensing-type transition. Applied Surface Science, 2018, 448, 489-497.	6.1	44
47	Low power-consumption CO gas sensors based on Au-functionalized SnO2-ZnO core-shell nanowires. Sensors and Actuators B: Chemical, 2018, 267, 597-607.	7.8	118
48	Superhydrophobic and oleophilic microâ€nano hierarchical Pdâ€decorated SiO 2 layers. Journal of the American Ceramic Society, 2018, 101, 3817-3829.	3.8	5
49	Facile fabrication of superhydrophobic surfaces from austenitic stainless steel (AISI 304) by chemical etching. Applied Surface Science, 2018, 439, 598-604.	6.1	126
50	Novel superamphiphobic surfaces based on micro-nano hierarchical fluorinated Ag/SiO2 structures. Applied Surface Science, 2018, 445, 262-271.	6.1	29
51	Gas sensing properties of standard soda-lime glass. Sensors and Actuators B: Chemical, 2018, 266, 344-353.	7.8	12
52	Resistive-based gas sensors for detection of benzene, toluene and xylene (BTX) gases: a review. Journal of Materials Chemistry C, 2018, 6, 4342-4370.	5.5	255
53	Sensing behavior to ppm-level gases and synergistic sensing mechanism in metal-functionalized rGO-loaded ZnO nanofibers. Sensors and Actuators B: Chemical, 2018, 255, 1884-1896.	7.8	100
54	SnO2 (n)-NiO (p) composite nanowebs: Gas sensing properties and sensing mechanisms. Sensors and Actuators B: Chemical, 2018, 258, 204-214.	7.8	115

#	Article	IF	CITATIONS
55	How shell thickness can affect the gas sensing properties of nanostructured materials: Survey of literature. Sensors and Actuators B: Chemical, 2018, 258, 270-294.	7.8	117
56	High-Performance Nanowire Hydrogen Sensors by Exploiting the Synergistic Effect of Pd Nanoparticles and Metal–Organic Framework Membranes. ACS Applied Materials & Interfaces, 2018, 10, 34765-34773.	8.0	135
57	Synthesis of Aligned TiO2 Nanofibers Using Electrospinning. Applied Sciences (Switzerland), 2018, 8, 309.	2.5	28
58	Facile synthesis and electrochemical properties of carbon-coated ZnO nanotubes for high-rate lithium storage. Ceramics International, 2018, 44, 18222-18226.	4.8	14
59	Electrowetting on dielectric (EWOD) properties of Teflon-coated electrosprayed silica layers in air and oil media and the influence of electric leakage. Journal of Materials Chemistry C, 2018, 6, 6808-6815.	5.5	19
60	Synthesis and Selective Sensing Properties of rGO/Metal-Coloaded SnO2 Nanofibers. Journal of Electronic Materials, 2017, 46, 3531-3541.	2.2	30
61	Extremely sensitive and selective sub-ppm CO detection by the synergistic effect of Au nanoparticles and core–shell nanowires. Sensors and Actuators B: Chemical, 2017, 249, 177-188.	7.8	63
62	Self-heating effects on the toluene sensing of Pt-functionalized SnO2–ZnO core–shell nanowires. Sensors and Actuators B: Chemical, 2017, 251, 781-794.	7.8	41
63	Optimization and gas sensing mechanism of n-SnO2-p-Co3O4 composite nanofibers. Sensors and Actuators B: Chemical, 2017, 248, 500-511.	7.8	116
64	Ultra-sensitive benzene detection by a novel approach: Core-shell nanowires combined with the Pd-functionalization. Sensors and Actuators B: Chemical, 2017, 239, 578-585.	7.8	43
65	Optimization of metal nanoparticle amount on SnO2 nanowires to achieve superior gas sensing properties. Sensors and Actuators B: Chemical, 2017, 238, 374-380.	7.8	30
66	Synthesis and gas sensing properties of membrane template-grown hollow ZnO nanowires. Nano Convergence, 2017, 4, 27.	12.1	17
67	Electrospun Metal Oxide Composite Nanofibers Gas Sensors: A Review. Journal of the Korean Ceramic Society, 2017, 54, 366-379.	2.3	90
68	Growth of Networked TiO2 Nanowires for Gas-Sensing Applications. Journal of Nanoscience and Nanotechnology, 2016, 16, 11580-11585.	0.9	10
69	Improvement of Toluene-Sensing Performance of SnO2 Nanofibers by Pt Functionalization. Sensors, 2016, 16, 1857.	3.8	21
70	Crystallinity dependent gas-sensing abilities of ZnO hollow fibers. Metals and Materials International, 2016, 22, 942-946.	3.4	11
71	Influence of hollowness variation on the gas-sensing properties of ZnO hollow nanofibers. Sensors and Actuators B: Chemical, 2016, 232, 698-704.	7.8	41
72	Highly Selective Sensing of CO, C ₆ H ₆ , and C ₇ H ₈ Gases by Catalytic Functionalization with Metal Nanoparticles. ACS Applied Materials & Interfaces, 2016, 8, 7173-7183.	8.0	75

#	Article	IF	CITATIONS
73	MOF-Based Membrane Encapsulated ZnO Nanowires for Enhanced Gas Sensor Selectivity. ACS Applied Materials & Interfaces, 2016, 8, 8323-8328.	8.0	346
74	Realization of ppm-level CO detection with exceptionally high sensitivity using reduced graphene oxide-loaded SnO ₂ nanofibers with simultaneous Au functionalization. Chemical Communications, 2016, 52, 3832-3835.	4.1	40
75	Effect of Au nanoparticle size on the gas-sensing performance of p-CuO nanowires. Sensors and Actuators B: Chemical, 2016, 222, 307-314.	7.8	81
76	Optimum shell thickness and underlying sensing mechanism in p–n CuO–ZnO core–shell nanowires. Sensors and Actuators B: Chemical, 2016, 222, 249-256.	7.8	64
77	Excellent Carbon Monoxide Sensing Performance of Au-Decorated SnO2 Nanofibers. Korean Journal of Materials Research, 2016, 26, 741-750.	0.2	19
78	Significance of the Nanograin Size on the H ₂ S-Sensing Ability of CuO-SnO ₂ Composite Nanofibers. Journal of Sensors, 2015, 2015, 1-7.	1.1	12
79	Remarkable Improvement of Gas-Sensing Abilities in p-type Oxide Nanowires by Local Modification of the Hole-Accumulation Layer. ACS Applied Materials & amp; Interfaces, 2015, 7, 647-652.	8.0	67
80	Growth and sensing properties of networked p-CuO nanowires. Sensors and Actuators B: Chemical, 2015, 212, 190-195.	7.8	76
81	Extraordinary Improvement of Gas-Sensing Performances in SnO ₂ Nanofibers Due to Creation of Local <i>p</i> – <i>n</i> Heterojunctions by Loading Reduced Graphene Oxide Nanosheets. ACS Applied Materials & Interfaces, 2015, 7, 3101-3109.	8.0	143
82	Striking sensing improvement of n-type oxide nanowires by electronic sensitization based on work function difference. Journal of Materials Chemistry C, 2015, 3, 1521-1527.	5.5	57
83	Realization of ppb-Scale Toluene-Sensing Abilities with Pt-Functionalized SnO ₂ –ZnO Core–Shell Nanowires. ACS Applied Materials & Interfaces, 2015, 7, 17199-17208.	8.0	87
84	Excellent gas detection of ZnO nanofibers by loading with reduced graphene oxide nanosheets. Sensors and Actuators B: Chemical, 2015, 221, 1499-1507.	7.8	112
85	Chemiresistive Sensing Behavior of SnO ₂ (<i>n</i>)–Cu ₂ O (<i>p</i>) Core–Shell Nanowires. ACS Applied Materials & Interfaces, 2015, 7, 15351-15358.	8.0	74
86	Bifunctional Sensing Mechanism of SnO ₂ –ZnO Composite Nanofibers for Drastically Enhancing the Sensing Behavior in H ₂ Gas. ACS Applied Materials & Interfaces, 2015, 7, 11351-11358.	8.0	143
87	Importance of the nanograin size on the H2S-sensing properties of ZnO–CuO composite nanofibers. Sensors and Actuators B: Chemical, 2015, 214, 111-116.	7.8	86
88	CuO/SnO ₂ Mixed Nanofibers for H ₂ S Detection. Journal of Nanoscience and Nanotechnology, 2015, 15, 8637-8641.	0.9	13
89	Evolution of grains to relieve additional compressive stress developed in Al–Mg alloy films during thermal annealing. Thin Solid Films, 2015, 595, 148-152.	1.8	1
90	A Novel Synthesis Route for Pt-Loaded SnO ₂ Nanofibers and Their Sensing Properties. Journal of Nanoscience and Nanotechnology, 2014, 14, 8253-8257.	0.9	4

#	Article	IF	CITATIONS
91	Dual Functional Sensing Mechanism in SnO ₂ –ZnO Core–Shell Nanowires. ACS Applied Materials & Interfaces, 2014, 6, 8281-8287.	8.0	125
92	TiO ₂ /ZnO Inner/Outer Double-Layer Hollow Fibers for Improved Detection of Reducing Gases. ACS Applied Materials & Interfaces, 2014, 6, 21494-21499.	8.0	68
93	Prominent Reducing Gas-Sensing Performances of <i>n</i> -SnO ₂ Nanowires by Local Creation of <i>p</i> – <i>n</i> Heterojunctions by Functionalization with <i>p</i> -Cr ₂ O ₃ Nanoparticles. ACS Applied Materials & amp; Interfaces, 2014, 6, 17723-17729.	8.0	101
94	A novel approach to improving oxidizing-gas sensing ability of p-CuO nanowires using biased radial modulation of a hole-accumulation layer. Journal of Materials Chemistry C, 2014, 2, 8911-8917.	5.5	35
95	Glucose Sensors Using Lipoic Acid Self-Assembled Monolayers. Journal of Sensor Science and Technology, 2014, 23, 295-298.	0.2	1
96	Change in Water Contact Angle on Electrospray-Synthesized SiO2Coated Layers by Plasma Exposure. Korean Journal of Materials Research, 2014, 24, 639-643.	0.2	0
97	Characterization of the crystallographic microstructure of the stress-induced void in Cu interconnects. Applied Physics Letters, 2008, 92, 141917.	3.3	12